Journal of Applied Fluid Mechanics, Vol. 10, No. 3, pp. 871-879, 2017.
Available online at www.jafmonline.net, ISSN 1735-3572, EISSN 1735-3645.
DOI: 10.18869/acadpub.jafm.73.240.26650

Steady MHD Flow of Nano-Fluids over a Rotating Porous Disk in the Presence of Heat Generation/Absorption: a Numerical Study using PSO

Z. Uddin[1†], R. Asthana[1], M. Kumar Awasthi [2] and S. Gupta[1]

[1]*SoET, BML Munjal University, Gurgaon, Haryana 123413, India.*
[2]*Department of Mathematics, UPES, Dehradun, India*

†*Corresponding Author Email: ziya_dd@rediffmail.com*

(Received June 7, 2016; accepted January 17, 2017)

ABSTRACT

In this paper, a numerical integration technique, based on particle swarm optimization is proposed to investigate the effects of internal heat generation/absorption, on MHD boundary-layer flow of different types of nano-fluids over a rotating disk with uniform suction. Thermo-physical properties are modeled based on a wide range of experimental data. In the model, effect of nature of base fluid, nature of nano-particle material, size of nano particle, concentration of nanoparticle in the base fluid, nano-thermal layer formed around the nano particle etc. are taken into consideration. The two dimensional non-linear partial differential equations governing the flow are reduced to a system of coupled non-linear ordinary differential equations by using similarity transformations. These non-linear equations have been solved by using shooting based integration technique along with particle swarm optimization. In this study, four different types of water bases nanofluids are compared with respect to heat transfer enhancement, and the effects of nano-particle concentration, nano-particle size and heat generation/absorption parameters are studied in detail. The effects of different parameters on the dimensionless velocity profile and temperature distribution are discussed graphically. It is found that out of the four nano fluids considered, the heat transfer rate for CuO water based nano fluid is highest. It is also concluded that small sized nano-particles, high suction and high heat absorption increase the heat transfer rate.

Keywords: MHD flow; Nano fluid; Porous disk; Heat absorption; Cooling; Particle swarm optimization; Numerical simulation.

1. INTRODUCTION

Fluid flow over a rotating disk has various applications in Industrial and engineering processes such as rotating machinery, lubrication, oceanography and computer storage devices, etc. Von Karman (1921) formulated this rotating disk problem and gave the transformation to convert the governing partial differential equations into ordinary differential equations. The theoretical and experimental investigation of such type of flow problems has attracted various researchers after the pioneer work of Karman (1921). Rotating disk problems have been successfully studied and used in cooling rotating machinery and generators for decades. Usha *et al*. (2004) analyzed the unsteady thin conducting liquid film of non-uniform thickness on a rotating disk which is cooled axisymmetrically from below. The rotationally symmetric flow over a rotating disk of an incompressible viscous fluid is analyzed by Chawla *et al*. (2009). The steady flow of an incompressible viscous fluid above an infinite rotating disk in a porous medium is studied by Attia (2009). Attia reported that, with the increase in porosity parameter the temperature and thickness of the thermal boundary layer increase. Anjali Devi *et al*. (2011) analyzed the radiation effects on hydro-magnetic flow due to a rotating disk, and reported that the rate of heat transfer increases with the increasing values of radiation parameter. Recently Griffiths (2015) studied the boundary-layer flow due to a rotating disk considering few generalised Newtonian fluid models. From literature surveyed, it is also observed that the presence of magnetic field also plays an important role on heat transfer rate and fluid flow characteristics. Uddin *et al*. (2013) studied the Hall and ion-slip effect on boundary layer flow of a micro polar fluid past a wedge in presence of magnetic field and concluded that in a micro polar fluid, the

Hall effect and increased magnetic field enhances the heat transfer rate significantly. Seth *et al*. (2015a), (2015b) and (2015c) also studied the Hall current effects on hydromagnetic convection flow under different heat generation/absorption conditions. Magneto hydrodynamic stagnation point flow and heat transfer on stretching sheet with chemical reaction and transpiration is studied by Mabood *et al*. (2015). The obtained results show that the flow field is substantially influenced by the presence of chemical reaction, transpiration, and magnetic field. The flow past a rotating disk in presence of magnetic field is also studied by various researchers. Arikoglu *et al*. (2006) formulated the problem to study the steady magneto-hydrodynamic (MHD) flow of a viscous, Newtonian and electrically conducting fluid over a rotating infinite disk with slip boundary condition and found that both the slip factor and the magnetic flux decrease the velocity in all directions and thicken the thermal boundary layer. Effects of thermal radiation on MHD and slip flow over a porous rotating disk with temperature dependent thermo-physical properties of fluid are analyzed by Osalusi (2007). Shrinking rotating disks have also been studied under different conditions. Turkyilmazoglu (2014) derived the solution for the fluid flow and heat transfer due to a shrinking rotating disk in presence of magnetic field and concluded that the heat transfer is reduced for low rotations and radial shrinking of the disk can overcome the wall heating. the effects of heat generation/absorption on the fluid flow and heat transfer characteristics under different flow configurations is also studied by various thermal science researchers (Rafael (2005), Uddin *et al*. (2014) and Ravindran *et al*. (2014). It is concluded from the numerical computations reported in the literature that the heat absorption enhances the skin friction, heat and mass transfer coefficients.

The thermal performance of the any cooling/heating system depends upon thermos-physical properties of the fluid flow involved in the process. Therefore, to improve the thermal performance the fluid with improved thermal properties has to be used. But the common fluids like water, ethylene glycol and oil etc. have low thermal conductivities. On the other hand metals and their oxide have high thermal conductivities compared to these fluids. A uniform dispersion of low concentration nano-size metal/metal-oxide particles into the base fluid can enhance the thermal conductivity; these fluids containing nano-size particles are called nano-fluids [Yu *et al*. (2003)]. This concept attracted various researchers towards nano-fluids, and various theoretical and experimental studies have been done to find the thermal performance using nano-fluids [Alsaedi *et al*. (2012), Uddin *et al*. (2013), Uddin (2015), Ganga *et al*. (2015) and Rashidi *et al*. (2013)]. It has been observed that the thermal conductivity of nano-fluids depends on the various factors e.g., particle material, base fluid material, particle volume fraction, particle size, particle shape, temperature, nano-particle Brownian motion, nano-particle-base fluid interfacial layers, and particle clustering etc. [Yu *et al*. (2003), Uddin *et al*. (2013)]. The effects of heat generation/absorption on stagnation point flow of nano-fluid over a surface with convective boundary conditions are studied by Alsaedi *et al*. (2012). In this numerical study Alsaedi analyzed the velocity, temperature and nanoparticle concentration profiles with respect to the Brownian motion, thermophoresis parameter, permeability parameter etc. Uddin (2015) obtained the solution for the MHD boundary layer flow of a nano-fluid past a wedge shaped wick used in heat pipe to draw the heat from a system. Recently Ganga *et al*. (2015) studied the MHD radiative boundary layer flow of nanofluid past a vertical plate with internal heat generation/absorption, viscous and ohmic dissipation effects. The studies involving the rotating disks under different conditions have been done by the researchers, but only a few theoretical/numerical studies of the nano fluid flow past rotating disks have been reported. Rashdi *et al*. (2013) applied the second law of thermodynamics to an electrically conducting incompressible nanofluid fluid flowing over a porous rotating disk in the presence of an externally applied uniform vertical magnetic field. In this study Rashidi *et al*. considered only the effect of nano particle concentration on the thermos-physical properties of the nano fluids. To the best of our knowledge, none of the study involves the rotating disks in presence of heat generation/absorption with nano-fluids considering the effect of nano particle size, nano liquid layer formed around the nano particle, nano particle concentration etc.

Therefore, the scope of the present work is to implement the appropriate empirical models for the properties of nano-fluids which satisfy a wide range of experimental data, and to study the effects of nano fluid type, nano paticle concentraition, nano particle size, heat generation on heat transfer and skin friction coefficients. To solve the non-linear differential equations governing the flow and heat transfer of nano-fluids over the rotating disk, a new methodology based on particle swarm optimization (PSO) has been considered.

2. MATHEMATICAL FORMULATION

The problem of steady, axially symmetric laminar flow of nano-fluid over a porous rotating disk under heat absorption/generation is considered. A uniform magnetic field is applied perpendicular to the surface of rotating disk. The z axis for the cylindrical coordinate system is taken perpendicular to the surface of the disk. *u, v* and *w* are the velocity components along the *r, Θ* and *z* directions respectively. The ambient temperature is T_∞ and the temperature of the disk is T_w. The physical model and coordinate system are shown in Fig. 1. Under these assumptions the equations governing the flow and heat transfer are given below.

Continuity equation:

$$\frac{\partial u}{\partial r}+\frac{u}{r}+\frac{\partial w}{\partial z}=0 \tag{1}$$

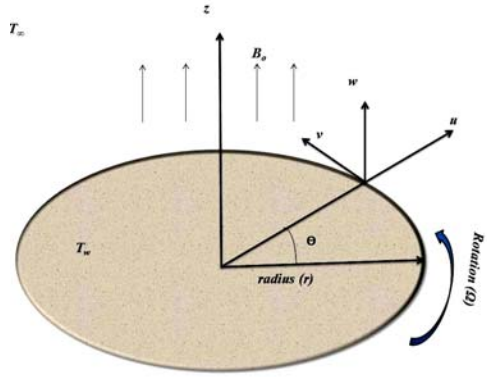

Fig. 1. Physical Model and coordinate system.

Momentum equations:

$$u\frac{\partial u}{\partial r}+w\frac{\partial u}{\partial z}-\frac{v^2}{r}+\frac{1}{\rho_{nf}}\frac{\partial p}{\partial r}=\nu_{nf}\left(\frac{\partial^2 u}{\partial r^2}+\frac{\partial^2 u}{\partial z^2}\right)-\frac{\sigma B_0^2 u}{\rho_{nf}} \tag{2}$$

$$u\frac{\partial v}{\partial r}+w\frac{\partial v}{\partial z}+\frac{uv}{r}=\nu_{nf}\left(\frac{\partial^2 v}{\partial r^2}+\frac{\partial^2 v}{\partial z^2}\right)-\frac{\sigma B_0^2 v}{\rho_{nf}} \tag{3}$$

$$u\frac{\partial w}{\partial r}+w\frac{\partial w}{\partial z}+\frac{1}{\rho_{nf}}\frac{\partial p}{\partial z}=\nu_{nf}\left(\frac{\partial^2 w}{\partial r^2}+\frac{\partial^2 w}{\partial z^2}\right) \tag{4}$$

Energy equation:

$$u\frac{\partial T}{\partial r}+w\frac{\partial T}{\partial z}=\frac{k_{nf}}{(\rho C_p)_{nf}}\left(\frac{\partial^2 T}{\partial r^2}+\frac{\partial^2 T}{\partial z^2}\right)+Q_0 \tag{5}$$

here Q_0 is heat generation/absorption and the sub script "*nf*" represents the thermal properties of nano fluid.

Boundary conditions are:

$$u=0,\quad v=r\Omega,\quad w=w_0,\quad T=T_w,\quad at\quad z=0,$$

$$u\to 0,\quad v\to 0,\quad P\to P_\infty,\quad T\to T_\infty,\quad at\quad z\to\infty, \tag{6}$$

Nanofluid properties:

$$\rho_{nf}=\phi\rho_p+(1-\phi)\rho_f \tag{7}$$

$$(\rho C_p)_{nf}=\phi(\rho C_p)_p+(1-\phi)(\rho C_p)_f \tag{8}$$

To consider the effect of nano particle size, nano particle concentration and nano-thermal layer formed by the fluid around the nano particle etc. and keeping the experimental validation of the thermo physical properties of nanofluids, appropriate models for effective viscosity and effective thermal conductivity of nanofluids are used. Following Uddin *et al*. (2013) the viscosity of nano fluid is given by:

$$\mu_{nf}=\frac{\mu_f}{1-34.87\left(d_p/d_f\right)^{-0.3}\phi^{1.03}} \tag{9}$$

$$d_f=0.1\left[\frac{6Mo}{N\pi\rho_{fo}}\right]^{1/3}$$

here d_f is the diameter of base fluid molecule, Mo is the molecular weight of the base fluid, N is the Avogadro number (N= 6.0223e+023) , and ρ_{fo} is the mass density of the base fluid calculated at the reference temperature. For water Mo=18.01528e-003 and ρ_{fo} =998.19

The effective thermal conductivity of nanofluids (Yu *et al*. (2003)) is given by:

$$k_{nf}=\left[\frac{k_{pe}+2k_f+2(k_{pe}-k_f)(1-\beta)^3\phi}{k_{pe}+2k_f-2(k_{pe}-k_f)(1+\beta)^3\phi}\right]k_f \tag{10}$$

$$k_{pe}=\gamma\left[\frac{2(1-\gamma)+(1-\beta)^3(1+2\gamma)}{-(1-\gamma)+(1+\beta)^3(1+2\gamma)}\right]k_f, \tag{11}$$

$$\gamma=\frac{k_{layer}}{k_p}$$

$$\beta=\frac{h}{r_p}$$

Here k_f is thermal conductivity of base fluid, r_p is radius of nano particle, d_p is diameter of nano particle, k_p is thermal conductivity of nano particle, h is the thickness of nano layer formed by the fluid particles around the nano particle, k_{layer} is the thermal conductivity of the nano layer. From the experimental results it is observed that $k_{layer}=100k_f$.

To simplify the equations (1-5) along with the boundary conditions (6), following non dimensional transformations are introduced:

$$\eta=\left(\Omega/\upsilon_{nf}\right)^{1/2}z,\qquad u=\Omega rF(\eta),\qquad v=\Omega rG(\eta),$$
$$w=\left(\Omega\upsilon_{nf}\right)^{1/2}H(\eta),$$

$$p-p_\infty=2\mu_{nf}\Omega P(\eta),\quad \theta(\eta)=(T-T_\infty)/(T_w-T_\infty)$$

and

$$Q=\frac{Q_0}{(T_w-T_\infty)\Omega} \tag{12}$$

Using the non-dimensional quantities (12) and the thermo-physical properties of nano-fluids (7-11), the transformed equations (1-6) are as follows:

$$H'+2F=0 \tag{13}$$

$$\frac{1}{(1-\phi+\phi\rho_s/\rho_f)}\left[\frac{1}{1-34.87\left(d_p/d_f\right)^{-0.3}\phi^{1.03}}\right]F'' \tag{14}$$
$$=HF'+F^2-G^2+MF$$

$$\frac{1}{(1-\phi+\phi\rho_s/\rho_f)}\left[\frac{1}{1-34.87\left(d_p/d_f\right)^{-0.3}\phi^{1.03}}\right]G'' \tag{15}$$
$$=HG'+2FG+MG$$

$$\frac{1}{\Pr}\frac{k_{nf}/k_f}{(\rho C_p)_{nf}/(\rho C_p)_f}\theta''-H\theta'+Q=0 \tag{16}$$

And boundary conditions are:

$$F(0)=0,\quad G(0)=0,\quad H(0)=W_s,\quad \theta(0)=1,$$

$$F(\infty)\to 0,\quad G(\infty)\to 0,\quad \theta(\infty)\to 0 \qquad (17)$$

where F, G, H and Θ are non-dimensional functions for velocities and temperature, η is non dimensional distance. M is magnetic field parameter, Pr is Prandtl number and Ws is suction parameter.

$$M=\sigma B_o^2 \Big/ \Omega\rho_{nf} \quad \Pr=\left(\upsilon\rho C_p\right)_f \Big/ k_f,\ W_s=w_o \Big/ \left(\Omega\upsilon_f\right)^{1/2}$$

The quantities of physical interest, such as heat transfer coefficient (Nusselt number) and skin friction coefficient are as follows:

$$Nu=\frac{rq_w}{k_f(T_w-T_\infty)},\quad C_f=\frac{\sqrt{\tau_{wr}^2+\tau_{w\phi}^2}}{\rho_f(\Omega r)^2}$$

where q_w, τ_{wr} and $\tau_{w\phi}$ are the surface heat flux, radial and transversal shear stresses at the surface of the disk, respectively and given by the formulae,

$$q_w=-k_{nf}(T)_{z=0},\qquad \tau_{wr}=\left[\mu_{nf}(u_z+w_\phi)\right]_{z=0},$$

$$\tau_{w\phi}=\left[\mu_{nf}\left(v_z+\frac{1}{r}w_\phi\right)\right]_{z=0},$$

Introducing non-dimensional parameters defined in Equation 12, we get the following non dimensional mathematical expressions for the Nusselt number and skin friction coefficients.

$$\mathrm{Re}^{-1/2}\,Nu=-\frac{k_{nf}}{k_f}\theta'(0),$$

$$\mathrm{Re}^{1/2}\,C_f=\frac{\sqrt{F'(0)^2+G'(0)^2}}{1-34.87\left(d_p/d_f\right)^{-0.3}\phi^{1.03}}\quad . \qquad (18)$$

Where $\mathrm{Re}=\Omega r^2/\upsilon_f$ is the local Reynolds Number.

3. METHOD OF SOLUTION

3.1 Particle Swarm Optimization (PSO)

Particle swarm optimization (PSO) [(Kennedy *et al*. (1995), Poli *et al*. (2007) and Rini *et al*. (2011)] is one of the evolutionary algorithms that simulates the behavior of Bird flocking and fish schooling etc. When a flock of birds searches for food, the birds find food through social cooperation with other birds in neighborhood. Initially all birds move randomly, but after a while all the birds follow a bird which is nearest to the food. Particle swarm optimization utilizes a population of particles that fly through the problem hyperspace with given velocities. In each iteration, the velocity of individual particle is stochastically adjusted according to its historical and the neighborhood best position. The particle best and the neighborhood best are derived according to a user defined fitness function. The movement of each particle naturally evolves to an optimal or near optimal solution. Every particle remembers its own previous best value as well as the neighborhood best. Then, all particles are informed about the most successful particle for further improvement in the solution.

In PSO, the term particle refers to a population member who is massless and volume-less that is subject to velocity and acceleration towards a better mode of behavior. Each particle keeps track of its coordinates in the problem space which are associated with the best solution (objective function to be optimized) achieved so far. This value is called '*pbest*'. The particle also keeps track of the best value obtained so far by any particle in the neighborhood. This value is called '*Ibest*'. At each time step, the particle swarm optimization changes the velocity of each particle towards its '*pbest*' and '*Ibest*'. In PSO a fitness function is defined which is to be optimized (minimize for the present case). Initially a number of random solutions of the problem are generated in the search space. In each iteration, the values of fitness function are calculated for each particle and two minimum values of the fitness function are found. The first value is named as 'pbest' and the second value is called 'Ibest'. Each particle's velocity and position are updated by the following equations.

$$v[\,]=\omega * v[\,]+\phi_p * rand\ ()*(pbest\ [\,]-x[\,])+\phi_g * rand\ ()*(Ibest\ [\,]-x[\,]) \qquad (19)$$

$$x[\,]=x[\,]+v[\,] \qquad (20)$$

Here, $x[\,]$ and $v[\,]$ are the particle position and velocity respectively. *rand( )* is a random number in the range [0,1]. ϕ_p, ϕ_g and ω are the positive parameters of PSO known as local weights and inertial weigh respectively. Large values of ω facilitates the global search while its small value facilitates the local search. To control the maximum velocities of the particles and for efficient working of PSO to search the global optima we took $\phi_p=\phi_g=1.49618$ and $\omega=0.7298$ (See Poli *et al*. (2007)).

A. Implementation of PSO

The non-linear differential equations (13)-(16) subjected to the boundary condition (17) constitute a boundary value problem. In order to solve these equations numerically, Runge-Kutta Fehlberg method with particle swarm optimization based shooting technique is applied. The ordinary differential equation (13)-(16) are first converted into a set of seven first-order simultaneous equations. To solve this system we require seven initial conditions but we have only four initial conditions. The initial condition for F', G' and θ' are not known. However few values of F, G and θ are known at the other end boundary $\eta\to\infty$. To find the solution of these coupled equations we

Table 1 Thermo-physical properties of base fluid and nano particles

Physical property	Base Fluid (water)	Cu	CuO	Al_2O_3	TiO_2
μ	0.0009	-	-	-	-
$k(W/mK)$	0.613	400	76.5	40	8.9538
$C_p(J/kgK)$	4179	385	540	765	711
$\rho(kg/m^3)$	997.1	8933	6320	3970	4250

Table 2 Comparison of F'(0) values at Pr=0.71

Q	M	W_s	*F'(0)*	
			Rashidi *et al*. [1]	Present
0	1	0	0.309237	0.309236
		-1	0.251039	0.251038
		-2	0.188718	0.188715
0.01	1	0	-	0.309212830704085
		-1	-	0.251026017749365
		-2	-	0.188710212150685
0.02	1	0	-	0.309212830723846
		-1	-	0.251026017252705
		-2	-	0.188710211734944

Table 3 Comparison of G'(0) values at Pr=0.71

Q	M	W_s	*-G'(0)*	
			Rashidi *et al*. [1]	Present
0	1	0	1.06907	1.069073
		-1	1.65709	1.657096
		-2	2.43137	2.431366
0.01	1	0	-	1.069090056096871
		-1	-	1.657096463596685
		-2	-	2.431362953432099
0.02	1	0	-	1.069090056130019
		-1	-	1.657096464086620
		-2	-	2.431362953050845

employed the numerical integration technique based on PSO where the end boundary conditions are utilized to produce unknown initial conditions under the convergence criteria of $Min = \sqrt{(F(\infty))^2 + G(\infty)^2 + \theta(\infty)^2} \le 10^{-8}$. In the numerical computation "infinity" is taken equal to 5, because the momentum and thermal boundary layer thicknesses are less than 5, and for large values of η, there was no significant change in the results. This signifies that $\eta \to \infty$ can be considered as $\eta \to 5$. To get the unknown initial conditions, the objective function (fitness function for PSO) to be minimized is: $Min = \sqrt{(F(\infty))^2 + G(\infty)^2 + \theta(\infty)^2}$. In PSO algorithm, an optimized solution is usually achieved in a number of iterations using a random approach. Therefore to get the solution of the problem by using the methodology discussed above, we ran a MATLAB code until it satisfies the condition $Min \le 10^{-08}$. For each iteration, the random population size is taken as 200.

4. RESULTS AND DISCUSSION

The computations have been carried out for four different type of water based nano-fluids under different conditions. The thermo-physical properties of pure water and pure Cu, CuO, Al_2O_3 and TiO_2 are given in Table 1.

The effects of various parameters involved in the problem on the velocity profiles, temperature distribution, heat transfer coefficient and skin friction coefficient have been calculated and presented in the form of graphs and tables.

To check the validity of formulation, The results are compared with previously published work under certain conditions and presented it in Tables 2, 3 and 4. This Table implies that the results are in good agreement with the earlier published work and it proves the validity of the proposed method. From tables 2 and 3 it is also clear that, with the increase

Table 4 Comparison of -Θ'(0) values at Pr=0.71

Q	M	W_s	*-Θ (0)*	
			Rashidi *et al*. [1]	Present
0	1	0	0.14667	0.146666
		-1	0.74586	0.745855
		-2	1.43098	1.430976
0.01	1	0	-	0.235534109708767
		-1	-	0.735789091026227
		-2	-	1.401647176807394
0.02	1	0	-	0.217515993020170
		-1	-	0.709497527412252
		-2	-	1.371260025671108

Table 5 Comparison between different nano fluids

Nano Fluid	$Re^{-1/2}Nu$	$Re^{1/2}C_f$
Cu+water	5.84219936268068	1.950082858778213
CuO+water	5.84924247721898	1.818464436451492
Al_2O_3+water	5.8188622224327	1.695577287044732
TiO_2+water	5.81734176305903	1.695577287044732

Table 6 Dependence of Nao particle concentration, nano particle diameter, heat generation/absorption parameter on Nusselt number and Skin Friction coefficient

	For CuO+Water nano fluid		$Re^{-1/2}Nu$	$Re^{1/2}C_f$
For dp=10 nm, Ws=-1;h=2 nm; Q=0.01;M=1	ϕ	0	5.897663107954863	1.676002773752976
		0.025	5.87422486593043	1.756726188079726
		0.05	5.849242480378193	1.8184644362043187
		0.075	5.821328798065954	1.8630677063018293
For Ws=-1;h=2 nm; $\phi = 0.05$; Q=0.01;M=1	dp	5nm	5.857109179273039	1.7744404746554168
		10nm	5.849242490786001	1.8184644358528608
		15nm	5.8490349259406	1.839743370802213
For Ws=-1; h=2 nm; dp=10 nm; $\phi = 0.05$; M=1	Q	-0.01	6.416301285768981	1.8184644775463774
		0	6.132770343753118	1.8184644475267624
		0.01	5.849242498844978	1.818464436504073
		0.02	5.565714596757242	1.8184644253333337

in magnitude of suction parameter, value of *F'(0)* decreases, whereas the value of *G'(0)* increases. Table 4 shows the effect of suction parameter on *"-Θ (0)"*. This Table demonstrates that with the increase in magnitude of suction parameter, there is a significant increase in*"-Θ'(0)"* and causes the increase in heat transfer rate.

The comparison among different type of nano-fluids with respect to Nusselt number and skin friction coefficients have also been done and given in Table 5. For the comparison the computation parameters are Ws=-1; dp=10 nm; $\phi = 0.05$; Q=0.01; M=1; h=2 nm; k_{layer}=100k_f.

From the table 5, it is clear that the value of Nusselt number is highest for CuO+ water nanofluid and smallest for TiO_2+water nano-fluid. The value of the skin friction coefficient is highest for Cu+water nano-fluid. To find the effect of different parameters viz. nano particle concentration, nano particle size, heat generation/absorption parameter etc, the computations have been done for CuO+Water nanofluid only and the results are presented in Table 6 and Fig. 2-10.

The effect of nano particle concentration on velocity profiles and temperature distribution is shown in figs. 2-5. Figs. 2 and 3 depict that with the increase in nano particle concentration the radial and tangential velocity decrease, whereas fig. 4 shows that the axial velocity of the nano fluid increases with the increase in nano particle concentration. Fig. 5 shows that with the increase in nano particle concentration the temperature also increases, and results in the thickening of thermal boundary layer thickness. From table 6, it is concluded that, for 10 nm sized nano particles the increase in nano particle concentration decreases the heat transfer rate, whereas the skin friction

coefficient increases.

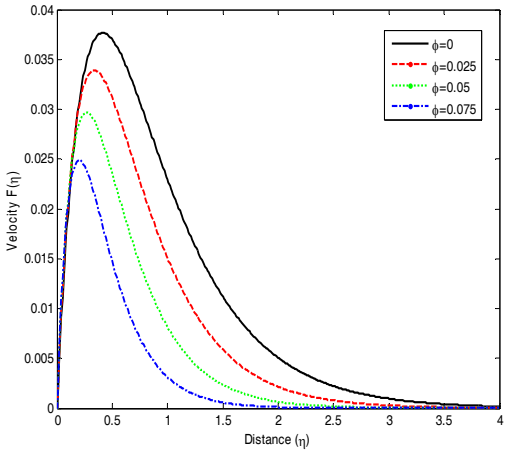

Fig. 2. Effect of nano-particle concentration on radial velocity for Ws=-1;h=2 nm; dp=10 nm; Q=0.01;M=1.

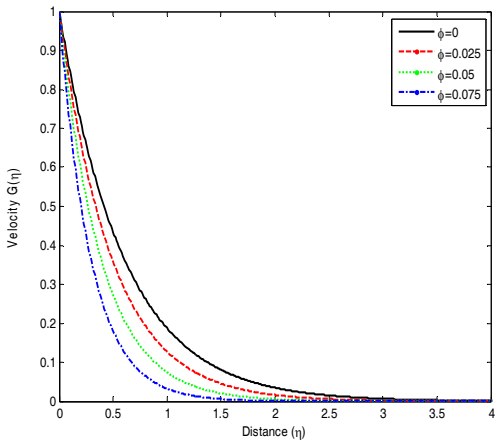

Fig. 3. Effect of nano-particle concentration on tangential velocity for Ws=-1;h=2 nm; dp=10 nm; Q=0.01;M=1.

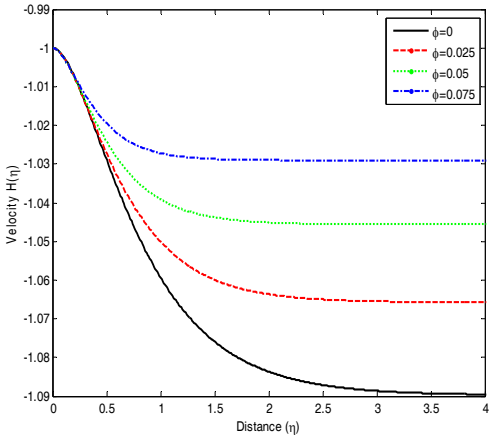

Fig. 4. Effect of nano-particle concentration on axial velocity for Ws=-1;h=2 nm; dp=10 nm; Q=0.01;M=1.

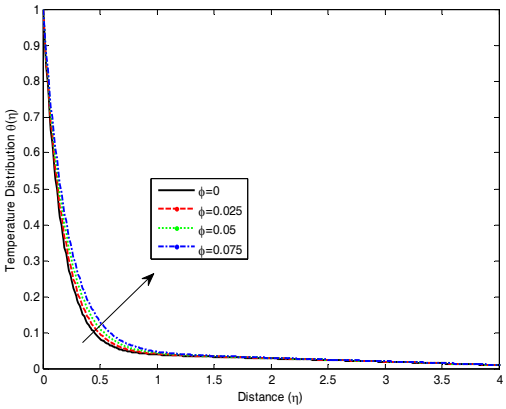

Fig. 5. Effect of nano-particle concentration on temperature distribution for Ws=-1;h=2 nm; dp=10 nm; Q=0.01;M=1.

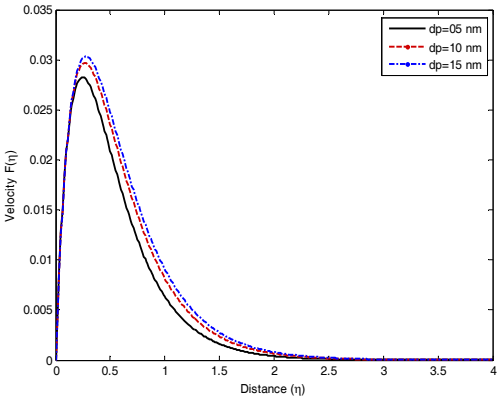

Fig. 6. Effect of nano-particle size on radial velocity for Ws=-1;h=2 nm; $\phi = 0.05$; Q=0.01;M=1.

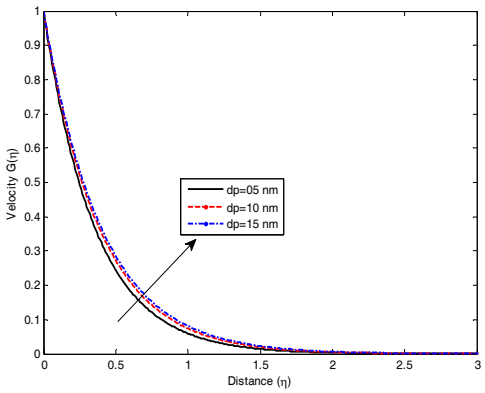

Fig. 7 Effect of nano-particle size on tangential velocity for Ws=-1;h=2 nm; $\phi = 0.05$; Q=0.01;M=1.

Figures 6-9 depicts the variation of velocity profiles and temperature distribution with nano particle size. It is clear from figs. 6, 7 and 8 that the radial and tangential velocities increase with the increase in particle diameter, whereas the axial velocity decreases. Since the skin friction depends upon the initial slope of radial and tangential velocity

profiles, therefore the increase in these velocity profiles with the increase in nano particle diameter results in increase in skin friction coefficient as given in table 6. Fig. 9 demonstrate that the increase in nano particle diameter decreases the temperature and causes the depletion of thermal boundary layer. Since the effective thermal conductivity of nano fluid decrease with the increase in nano particle diameter, therefore the heat transfer rate also decreases with the increase in nano particle diameter, as shown in table 6.

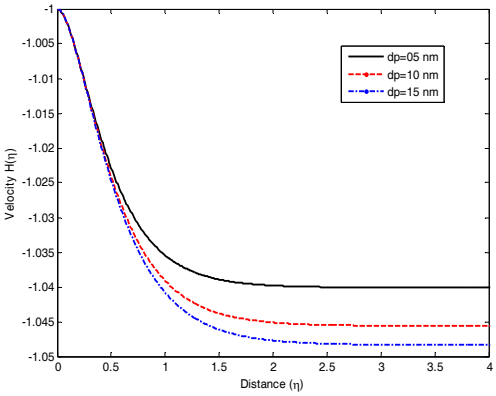

Fig. 8. Effect of nano-particle size on axial velocity for Ws=-1;h=2 nm; dp=10 nm; Q=0.01;M=1.

The effect of heat generation/absorption parameter on temperature distribution can be visualized in fig. 10. Positive values of "Q" in the figure are representing the heat generation and negative values are corresponding to heat absorption. From figure it is clear that as heat generation increases the thermal boundary layer thickness increases and heat absorption reduces the thermal boundary layer thickness. Increase in heat absorption means that the heat is withdrawn from the system by some means. This is the reason why increase in heat absorption parameter results in decrease in thermal boundary layer thickness and increase in heat transfer rate (as given in table 6).

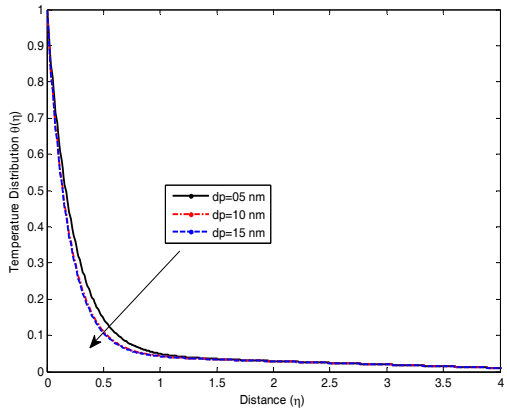

Fig. 9. Effect of nano-particle size on temperature distribution for Ws=-1;h=2 nm; dp=10 nm; Q=0.01;M=1.

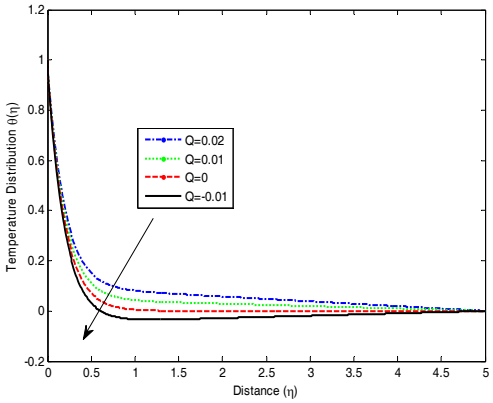

Fig. 10. Effect of heat generation/absorption parameter on temperature distribution for Ws=-1; h=2 nm; dp=10 nm; $\phi = 0.05$; M=1.

5. CONCLUSION

Steady MHD flow of nano-fluids over a rotating porous disk in presence of heat generation/absorption is studied numerically using a novel approach of particle swarm optimization along with Runge-Kutta Fehlberg method. It is observed that heat transfer and skin friction coefficient for the geometry discussed in this paper depend on various factors. viz., nano particle concentration in base fluid, nano particle diameter, heat generation/absorption, suctions velocity etc. From the present study it is concluded that:

- For Cu+Water nano fluid the value of skin friction is highest and for TiO2+Water nano it is least. The value of skin friction for CuO+Water nano fluid is in between these two nano fluids. At the same time the heat transfer rate is maximum in case of CuO+Water nano fluid. Therefore, it is a good option to use CuO+Water nano fluid in such type of configuration.
- The heat transfer rate is highest for small sized nano particles and at the same time skin friction is least. Therefore it can be concluded that, for practical applications related to thermal industry the best nano fluid is one with smallest nano size particle.
- Heat absorption and suction velocity also play an important role in heat transfer rate. More suction and more absorption enhance heat transfer rate.

REFERENCES

Alsaedi, A., M. Awais and T. Hayat (2012). Effects of heat generation/absorption on stagnation point flow of nanofluid over a surface with convective boundary conditions. *Communications in Nonlinear Science and Numerical Simulation*, 17(11), 4210–4223.

Anjali Devi, S. P. and R. Uma Devi (2011). On hydromagnetic flow due to a rotating disk with

radiation effects. *Nonlinear Analysis: Modelling and Control.* 16(1), 17–29.

Arikoglu, A. and I. Ozkol (2006). On the MHD and slip flow over a rotating disk with heat transfer. *Int. J. Numerical Methods for Heat & Fluid Flow.* 16(2), 172–184.

Attia, H. A. (2009). Steady Flow over a Rotating Disk in Porous Medium with Heat Transfer, *Nonlinear Analysis: Modelling and Control*. 14(1), 21–26.

Chawla, S. S., P. K. Srivastava and A. S. Gupta (2009). Rotationally symmetric flow over a rotating disk, *Int J non linear mech.* 44(7), 717–726.

Ganga, B., S. M. Yusuff Ansari , N. Vishnu Ganesh and A. K. Abdul Hakeem (2015). MHD radiative boundary layer flow of nanofluid past a vertical plate with internal heat generation/absorption, viscous and ohmic dissipation effects. *J Nigerian Math Soc.*

Griffiths, P. T. (2015). Flow of a generalised Newtonian fluid due to a rotating disk, *J Non-Newtonian Fluid Mechanics*. 221, 9–17.

Karman, T. V. (1921). Uber laminare und turbulente reibung. *ZAMM*, 1(4), 233–235.

Kennedy, J. and R. Eberhart (1995). Particle Swarm Optimization, Proc. IEEE International Conf. on Neural Networks, IEEE Service Center, Piscataway, NJ, Perth, Australia. 1942.

Khan, N. A., S. Aziz and N. A. Khan (2014). Numerical Simulation for the Unsteady MHD Flow and Heat Transfer of Couple Stress Fluid over a Rotating Disk. *PLoS ONE* 9(5).

Mabood, F., W. A.Khan and A. I. M. d. Ismail (2015). MHD stagnation point flow and heat transfer impinging on stretching sheet with chemical reaction and transpiration. *Chemical Engg. Journal.* 231(1), 430-437.

Osalusi, E. (2007). Effects of thermal radiation on MHD and slip flow over a porous rotating disk with variable properties. *Rom. Journ. Phys.* 52(3–4), 217–229.

Poli, R., J. Kennedy and T. Blackwell (2007). Particle swarm optimization: An overview. *Swarm Intell*, 33-57.

Rafael, C. (2005). Flow and heat transfer of a fluid through a porous medium over a stretching surface with internal heat generation/absorption and suction/blowing. *Fluid Dyn. Res*. 37(4), 231-245.

Rashidi, M. M., S. Abelman and N. Freidooni Mehr (2013). Entropy generation in steady MHD flow due to a rotating porous disk in a nanofluid. *Int J Heat Mass Transfer*, 62, 515-525.

Ravindran, R., M. Ganapathirao and I. Pop (2014). Effects of chemical reaction and heat generation/absorption on unsteady mixed convection MHD flow over a vertical cone with non-uniform slot mass transfer. *Int J Heat Mass transfer*, 73, 743-751.

Rini, D. P., Shamsuddin, S. M. and S. S. Yuhaniz (2011). Particle Swarm Optimization: Technique, System and Challenges. *Int. J. Comp. Applications*, 14(1), 19-27.

Seth ,G. S., S.Sarkar, S. M. Hussain and G. K. Mahato (2015a). Effects of Hall current and rotation on hydromagnetic natural convection flow with heat and mass transfer of a heat absorbing fluid past an impulsively moving vertical plate with ramped temperature. *J. Appl. Fluid Mech.* 8(1), 159-171.

Seth, G. S., B. Kumbhakar and R. Sharma (2015c). Unsteady hydromagnetic natural convection flow of a heat absorbing fluid within a rotating vertical channel in porous medium with Hall effects. *J. Appl. Fluid Mech.* 8(4), 767-779.

Seth, G. S., R. Sharma and S. Sarkar (2015b). Natural convection heat and mass transfer flow with Hall current, rotation, radiation and heat absorption past an accelerated moving vertical plate with ramped temperature. *J. Appl. Fluid Mech.* 8(1), 7-20.

Turkyilmazoglu, M. (2014). MHD fluid flow and heat transfer due to a shrinking rotating disk. *Computer and fluids*, 90(10), 51-56.

Uddin, Z. (2015). MHD Boundary Layer Flow of a Nano Fluid Past a Wedge Shaped Wick in Heat Pipe. *International Journal of Mechanical, Aerospace, Industrial and Mechatronics Engineering*, 9(5), 681-685.

Uddin, Z. and M. Kumar (2013). Hall and ion-slip effect on MHD boundary layer flow of a micro polar fluid past a wedge, *Scientia Iranica,* 20 (3), 467-476.

Uddin, Z. and S. Harmand. (2013). Natural convection heat transfer of nanofluids along a vertical plate embedded in porous medium. *Nanoscale research letters*, 8(64).

Uddin, Z., M. Kumar and S. Harmand (2014). Influence of thermal radiation and heat generation/absorption on MHD heat transfer flow of a micropolar fluid past a wedge considering hall and ion slip currents. *Thermal Science*. 18(2), S489-S502.

Usha, R and R. Ravindran (2004). Analysis of cooling of a conducting fluid film of non-uniform thickness on a rotating disk. *Int J non linear mech.* 39(1), 153-164.

Yu, W. and S. U. S. Choi (2003). The role of interfacial layers in the enhanced thermal conductivity of nanofluids: A renovated Maxwell model. *Journal of Nanoparticle Research*. 5, 167–171.